Analytical Sciences
https://doi.org/10.1007/s44211-026-00979-x

ORIGINAL PAPER

Two-color, laser-induced fluorometry for evaluating the efficiency of click chemistry-based labeling of extracellular vesicles

Arisa Takaya[1] · **Takashi Kaneta**[1]

Received: 21 July 2026 / Accepted: 16 October 2026
© The Author(s) 2026

Abstract
Extracellular vesicles (EVs), including exosomes, have attracted considerable attention as promising biomarkers for the early diagnosis and prognosis of cancer. In this study we evaluated the efficiency of a click chemistry-based EV labeling method using a two-color laser-induced fluorometry (LIF) system. During cell culture, cellular membranes were metabolically functionalized with azide groups, and the released EVs were subsequently labeled with Cy5 via click chemistry. The collected EVs were then stained with a phycoerythrin-conjugated anti-CD63 antibody (PE-anti-CD63) to achieve dual labeling. A two-color LIF system equipped with 488- and 635-nm lasers was used to distinguish Cy5-labeled, CD63-positive EVs from Cy5-unlabeled, CD63-positive EVs. Because PE and Cy5 are selectively excited at 488 and 635 nm, respectively, Cy5-labeled, CD63-positive EVs generated coincident dual-color fluorescence, whereas Cy5-unlabeled, CD63-positive EVs emitted fluorescence only upon 488-nm excitation. Using this platform, we investigated the effect that serum concentration in the culture medium exerts on click-chemistry labeling efficiency for CD63-positive EVs. The highest labeling efficiency for both HeLa and A549 cells was obtained in medium supplemented with 10% fetal bovine serum. These findings demonstrate the utility of the proposed two-color LIF system for quantitatively evaluating the click-chemistry labeling efficiency of CD63-positive EVs under different cell-culture conditions.

Keywords Extracellular vesicle · Exosome · Laser-induced fluorescence · Click chemistry · Fluorescent labeling

Introduction

Exosomes are a class of extracellular vesicles (EVs) secreted by biological cells and are present in various biofluids. They attracted widespread attention following the discovery of microRNA (miRNA) within these vesicles in 2007 [1]. Subsequently, Kahlert et al. and Thakur et al. identified DNA in serum exosomes from pancreatic cancer patients and in exosomes derived from three different cancer models, respectively [2, 3]. Together, these studies demonstrated that exosomes carry diverse biomolecules such as DNA, mRNA, miRNA, proteins, enzymes, and lipids, and mediate intercellular communication by transferring these cargoes to recipient cells. Such communication has been implicated in cancer progression and metastasis. Consequently, exosomes have emerged as promising biomarkers for the early diagnosis and prognosis of cancer [4–6].

Analytical methods for exosomes have been actively developed because their comprehensive characterization is expected to facilitate the diagnosis and treatment of various diseases. Because exosomes cannot be directly observed by conventional optical microscopy, efficient labeling and tracking strategies are essential for both in vitro and in vivo studies. Fluorescence labeling is one of the most widely used approaches because of the high sensitivity of fluorescence detection. The most common strategy employs fluorescently labeled antibodies against exosomal marker proteins such as CD9, CD63, and CD81. This approach enables the identification and analysis of specific exosome populations and has been widely applied in flow cytometry [7] and nanoparticle tracking analysis [8]. Alternatively, membrane-targeting fluorescent probes can non-specifically label EVs, which allows detection of the total EV population [9, 10]. Other approaches employ either membrane-targeting dyes or amino-reactive fluorophores to label EVs

✉ Takashi Kaneta
kaneta@okayama-u.ac.jp

[1] Department of Chemistry, Okayama University, 3-1-1 Tsushimanaka, Kita-ku, Okayama 700-8530, Japan

Published online: 28 October 2026

through interactions either with membrane lipids or surface proteins [11].

Smyth et al. developed a strategy for metabolically labeling cell membranes followed by fluorescent labeling of the EVs released from these cells using click chemistry [12]. Click chemistry provides a highly efficient and bioorthogonal means of introducing fluorescent labels under mild reaction conditions. Using this strategy, Son et al. demonstrated real-time tracking of exosomes both in vitro and in vivo [13]. Furthermore, several studies have reported the functionalization of exosomes through click chemistry-based reactions [14, 15]. Although click chemistry enables selective labeling of metabolically modified EVs while minimizing disruption of their biological properties, no study has quantitatively evaluated its labeling efficiency. Such quantitative evaluation is essential for optimizing labeling conditions and for the reliable application of click chemistry to EV analysis.

To address this issue, in the present study we proposed a method for quantitatively evaluating the proportion of click chemistry-labeled EVs within an EV sample. Two donor cancer cell lines, HeLa and A549, were metabolically labeled using the click chemistry-based approach reported by Son et al. [13], and the released EVs were collected by conventional ultracentrifugation and polymer-based precipitation with a commercial product, ExoQuick-TC. Therefore, the isolated samples contained a mixture of unlabeled and Cy5-labeled EVs, with the latter emitting fluorescence upon 635-nm excitation. CD63-positive EVs were subsequently labeled with a phycoerythrin-conjugated anti-CD63 antibody, which emitted fluorescence upon 488-nm excitation. Using a two-color laser-induced fluorometry (LIF) system previously developed by our group [16], we distinguished Cy5-labeled, CD63-positive EVs from Cy5-unlabeled, CD63-positive EVs, which thereby enabled a quantitative evaluation of the efficiency for click chemistry-based labeling.

While single-particle analytical platforms such as nano-flow cytometry (nano-FCM) have emerged for EV characterization, detecting small EVs (< 100 nm) or low-abundance surface markers often remains challenging without specialized signal amplification or particle-enlargement steps [17, 18]. Our two-color LIF approach provides a straightforward means for simultaneous dual-color fluorescence detection to quantitatively evaluate click-chemistry labeling efficiency on immunologically defined EV subpopulations without the need for complex particle-modifying procedures.

Experimental

Materials

Ultrapure water was obtained using a Milli-Q system (Millipore, Tokyo, Japan). Chloroform, 1 M hydrochloric acid, and 1 M sodium hydroxide solutions were purchased from the Fujifilm Wako Pure Chemical Corporation (Osaka, Japan). *N*-Azidoacetyl-D-mannosamine (Ac4ManNAz) and dibenzylcyclooctyne-conjugated cyanine 5 (DBCO-Cy5; maximum absorbance: 646 nm, maximum emission: 661 nm) were purchased from Sigma-Aldrich Japan (Tokyo, Japan). GlutaMAX, Dulbecco's Modified Eagle Medium (DMEM, high glucose), fetal bovine serum (FBS), antibiotic-antimycotic, 0.05% trypsin-EDTA, and Dulbecco's phosphate-buffered saline (DPBS) were obtained from Gibco (Thermo Fisher Scientific, Tokyo, Japan). Phycoerythrin-conjugated anti-CD63 antibody (PE-anti-CD63, cat. no. IM1914U) was purchased from Beckman Coulter (CA, USA). HeLa cells (human cervical cancer cells) and A549 cells (human alveolar basal-cell carcinoma cells) were obtained from the JCRB Cell Bank (Tokyo, Japan).

In this study, we defined individual EVs and particles as follows: CD63-positive EVs are the total population of EVs expressing CD63, regardless of Cy5 labeling status; Cy5-labeled, CD63-positive EVs are the subpopulation of CD63-positive EVs exhibiting Cy5 fluorescence intensity above the optical detection limit; and Cy5-unlabeled, CD63-positive EVs are the subpopulation of CD63-positive EVs with Cy5 fluorescence below the detection limit. Cy5-labeled, CD63-negative particles indicate all detected events/particles that do not express CD63 above the detection threshold. The Cy5-labeled, CD63-negative particles possibly include both EVs that do not express CD63 above the detection threshold and small cell debris different from EVs.

Apparatus

The configuration of the detection system was similar to that described in our previous studies using a square capillary [16, 19]. Briefly, two lasers operating at wavelengths of 488 nm (20 mW, BioRay laser, Edmund Optics, Tokyo, Japan) and 635 nm (6 mW, semiconductor laser, Sigma Koki, Tokyo, Japan) were shaped into sheet-like beams using cylindrical lenses. These beams were then focused at distinct positions within a square capillary (outer diameter: 363 μm; inner diameter: 75 μm; length: 60 cm; Molex, Kanagawa, Japan). The 488-nm laser beam was shaped to a width of 70 μm and a thickness of 30 μm, whereas the 635-nm beam measured 140 μm in width and 50 μm in thickness. The two laser beams passed through separate regions

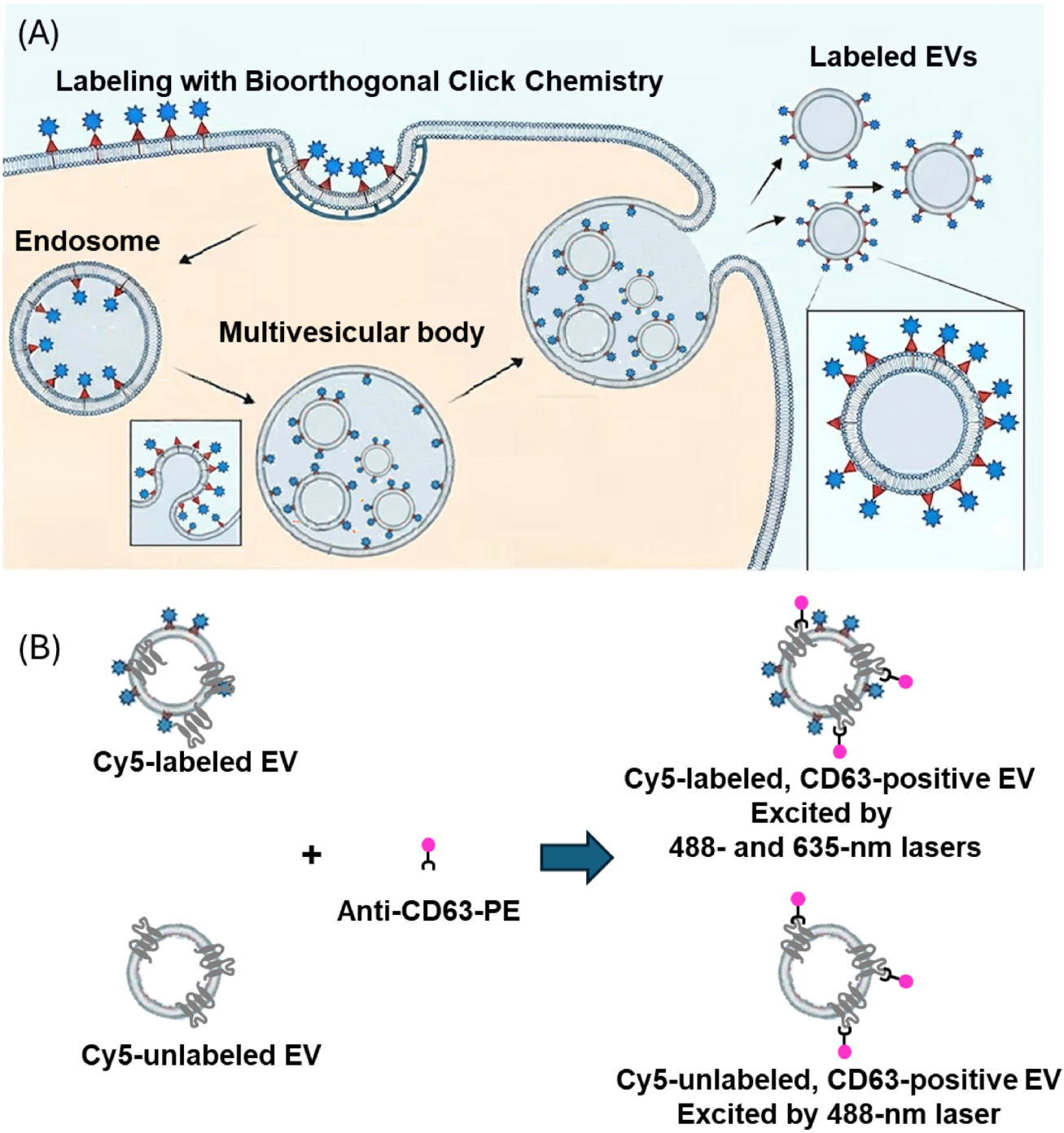


Fig. 1 Schematic illustration of exosome labeling. **A** Labeling with bioorthogonal click chemistry and **B** Labeling of EVs with anti-CD63 antibody conjugated with phycoerythrin (Anti-CD63-PE)

within the detection window without overlapping. A notch filter (StopLine, 488/532/635, OD 4 for each wavelength; Opto-Line, Inc., Saitama, Japan) positioned in front of an ORCA-Flash 2.8 CMOS camera (Hamamatsu Photonics, Shizuoka, Japan) was used to block scattered laser light. Fluorescence at the detection window was observed through an optical microscope equipped with a 20× objective lens and recorded using the camera. Image analysis was conducted using HCImage software (Hamamatsu Photonics).

The reliability of the system as a quantitative analytical platform under defined flow rate and acquisition time parameters was validated in our previous report using fluorescently labeled liposomes [16, 19]. Because the platform selectively detects marker-positive fluorescent EVs rather

than total physical particles, system accuracy relies on event counting that is relative to the sample concentration.

Click chemistry-based labeling and collection of EVs

Click-chemistry-labeled EVs were prepared according to a previously reported protocol with minor modifications [13]. A schematic illustration of the click chemistry-based labeling process is shown in Fig. 1A. The cell surface was initially modified with Ac4ManNAz and subsequently reacted with DBCO-Cy5 to form a Cy5-modified cell membrane. This labeled membrane underwent endocytosis to form endosomes, which was followed by the generation of multivesicular bodies and the release of Cy5-labeled EVs (Fig. 1A).

HeLa or A549 cells were cultured at 37 °C under a 5% CO_2 atmosphere in DMEM supplemented with 10% (v/v) fetal bovine serum (FBS) and antibiotic-antimycotic. The cells were cultured in 10-cm diameter petri dishes until approximately 100% confluence was reached. To subculture or treat the cells, the culture medium was removed, and the cells were detached by adding 1 mL of 0.05% trypsin-EDTA, which was followed by incubation at 37 °C for 5 min. The detached cells were suspended by adding 9 mL of the culture medium, and 9 mL of this cell suspension then was transferred to a new petri dish. Following the addition of 100 µL of 1.2 mM Ac4ManNAz to the dish, the cells were incubated for 24 h. The cells were then reacted with 242 µL of 0.41 mM DBCO-Cy5 for 1 h in the incubator. Subsequently, the medium was removed, and the cells were washed twice with 4 mL of DPBS. Finally, the cells were incubated for another 24 h in culture media containing specified concentrations of FBS (0, 5, 10, or 15%).

EVs were isolated from the collected culture media using ExoQuick-TC (System Biosciences, LLC, Palo Alto, CA) according to the manufacturer's protocol. While individual CD63-positive EVs can be detected using our single-particle LIF setup, sample concentration via ExoQuick-TC was incorporated prior to measurement to secure a sufficient particle count of the low-abundance Cy5-labeled EVs per unit volume, thereby ensuring reliable statistical evaluation of labeling efficiency. Initially, 5 mL of the culture medium was centrifuged at 2,580 × *g* for 15 min to remove cells and cellular debris. Then, 1 mL of ExoQuick-TC was added to the supernatant. The mixture was let stand in a refrigerator at 4 °C for 12 h, which then was followed by centrifugation at 1,500 × *g* for 30 min at 4 °C to obtain an EV pellet at the bottom of the centrifuge tube.

The collected EV pellet was resuspended in 100 µL of ultrapure water by vortex mixing for 10 s with subsequent sonication for 20 s. Short-term sonication efficiently dispersed EV aggregates, whereas prolonged sonication risked disrupting the vesicle structures; the maximum yield of dispersed EVs was achieved with a sonication time of 10 to 30 s (Fig. 2). To label all CD63-positive EVs, a 100-µL aliquot of the dispersed EV suspension was mixed with 2 µL of PE-anti-CD63 and shaken at 100 rpm for 1 h at room temperature. To finalize the reaction, the mixture was stored at 4 °C for 1 h. As illustrated in Fig. 1B, two types of CD63-positive EVs are present in the resultant mixture: one stained once with PE-anti-CD63 (Cy5-unlabeled, CD63-positive EVs) and the other stained twice with Cy5 and PE-anti-CD63 (Cy5-labeled, CD63-positive EVs).

Following this dual-labeling procedure, the sample contained a mixture of Cy5-unlabeled, CD63-positive EVs, Cy5-labeled, CD63-positive EVs, and CD63-negative EVs.

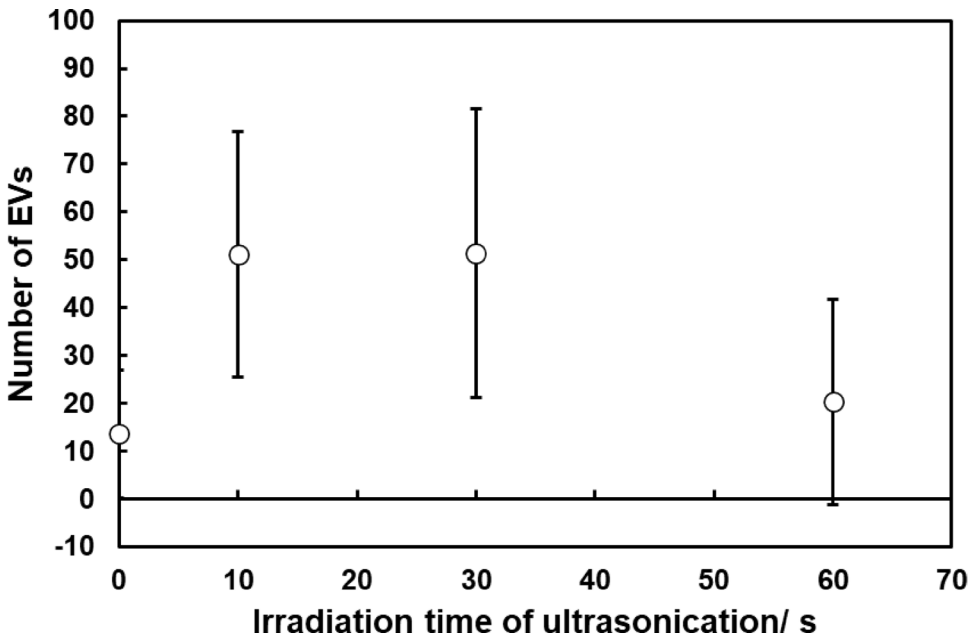


Fig. 2 Effect of time for ultrasonic irradiation on the counted number of EVs. The EVs labeled by bioorthogonal click chemistry were detected using a 635-nm laser

Because CD63-negative EVs do not generate a fluorescent signal under 488-nm excitation, they were excluded from detection in our system. Therefore, only the Cy5-labeled, and Cy5-unlabeled, CD63-positive EVs were selectively counted using the two-color LIF system by manually introducing the final suspension into the square capillary via syringe. To verify that FBS-derived EVs do not interfere with event detection, cell-free culture medium containing FBS was processed and analyzed using the same protocol and anti-CD63 antibody staining conditions as a negative control. We confirmed that no CD63-positive events above the background threshold were detected in the cell-free, FBS-containing medium.

Potential interference from unbound antibodies and membrane fragments is a shared limitation among fluorescence-based single-particle analytical platforms, which includes the use of flow cytometry. To ensure reliable signal discrimination, the experimental parameters were thoroughly optimized. Although unbound fluorophore-conjugated antibodies contribute to the baseline background fluorescence within the excitation volume (e.g., under 488-nm laser illumination), the antibody concentration was systematically optimized such that the fluorescence pulse from a single antibody-bound EV remains distinctly higher than the background noise floor [16, 19]. Additionally, gentle sample handling minimized vesicle disruption.

Results and discussion

Optimization of culture conditions and dual-color detection of EVs

In preliminary experiments, we attempted to label EVs via the click chemistry-based method using HeLa cells under experimental conditions reported in the literature [13]. The procedure reported in the literature utilized a serum-free medium containing 1% GlutaMAX, however, and no Cy5-labeled EVs were detected under these recommended conditions. This lack of a detectable signal could be attributed to reduced EV production and/or to diminished metabolic activity under serum-starved conditions. Consequently, we investigated the effect of adding serum to the 1% GlutaMAX medium, because serum supplementation is widely used to maintain cancer cell proliferation and metabolic activity.

When the cells were cultured in medium containing 10% FBS, fluorescent EVs became clearly detectable. Specifically, Cy5-labeled EVs were successfully observed in the capillary upon 635-nm excitation. These findings suggest that serum supplementation promotes cellular activity, which could increase EV production and improve the detectability of click-labeled EVs. Therefore, serum supplementation in the culture medium appears to be an important factor for increasing EV yields from donor cells.

To differentiate intact vesicular structures from small non-specific particles such as cellular debris, the collected EVs were counterstained with PE-anti-CD63. Accordingly, to remain consistent with the ISEV recommendations, the term “CD63-positive EVs” is used throughout this report for vesicles that exhibited fluorescence upon 488-nm excitation, rather than referring to them as exosomes. While the transmembrane protein CD63 is a widely accepted marker for EVs, the International Society for Extracellular Vesicles (ISEV) recommends that exosomes be identified by at least three positive marker proteins and one negative marker protein [20]. Because current isolation techniques cannot completely segregate true exosomes from other co-isolated EV subpopulations in a mixture, we strictly adopted the term “CD63-positive EVs” instead of “exosomes” throughout our quantitative analysis to ensure scientific accuracy.

The principle for discriminating between Cy5-labeled, and unlabeled, CD63-positive EVs is illustrated in Fig. 3. EVs stained with PE-anti-CD63 emitted fluorescence upon 488-nm excitation, whereas EVs labeled with both PE and Cy5 generated fluorescence signals at both the 488- and 635-nm excitation regions. Representative trajectories of individual CD63-positive EVs are shown in Fig. 4. A CD63-positive EV detected at 0.2 s in the upstream 488-nm excitation region subsequently generated Cy5 fluorescence while passing through the downstream 635-nm excitation region during the 0.6–1.0 s interval, which indicated successful click-chemistry labeling. By contrast, another CD63-positive EV detected at 1.0 s in the upstream excitation region produced no detectable Cy5 fluorescence during its subsequent passage through the downstream excitation region (1.2–1.8 s), which indicated that it was not labeled. Because EVs migrated through the capillary at a constant velocity, the transit time between the two excitation regions enabled reliable assignment of the upstream and downstream fluorescence signals to the same particle. These representative trajectories demonstrate that the developed dual-color LIF system reliably distinguishes Cy5-labeled, CD63-positive EVs from Cy5-unlabeled, CD63-positive EVs at the single-particle level. Control measurements using cell-free FBS-containing medium confirmed the absence of detectable CD63-positive events above the threshold [16, 17], which indicated that FBS-derived EVs neither cross-reacted with the anti-CD63 antibody nor interfered with the single-EV evaluation of Cy5- and CD63-positive events in our assay.

Thus, the proposed dual-laser platform successfully discriminates between Cy5-labeled, CD63-positive EVs and Cy5-unlabeled, CD63-positive EVs. By tracking the coincident passage of individual vesicles through the two excitation regions, the system enables direct quantification of

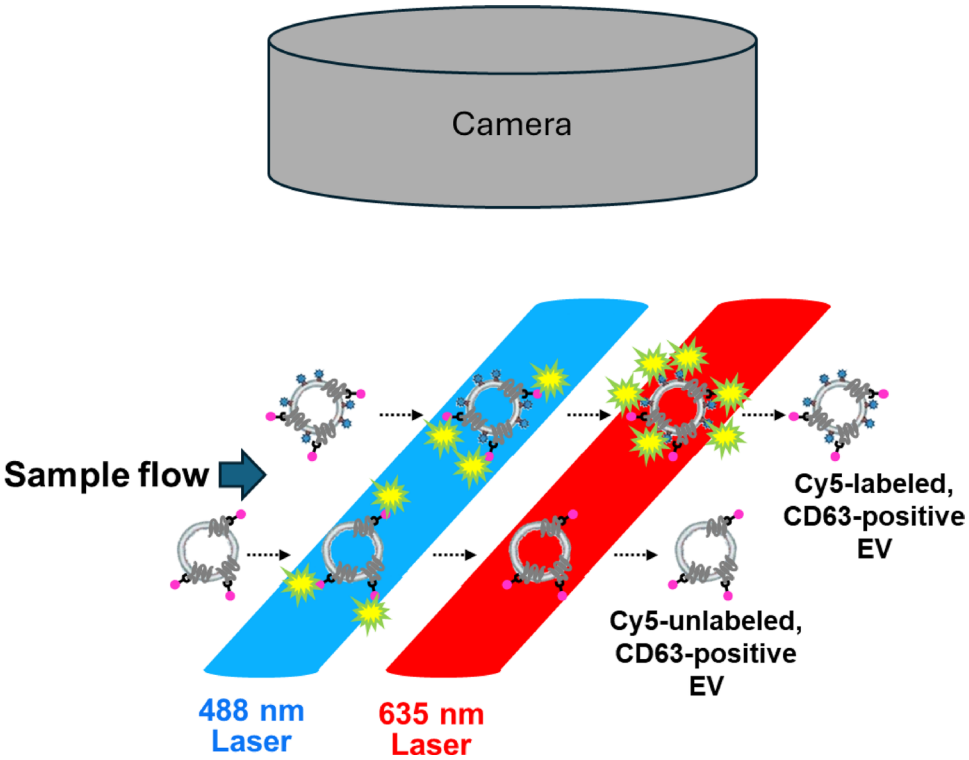


Fig. 3 Schematic illustration of discrimination between Cy5-labeled, CD63-positive EV and Cy5-unlabeled, CD63-positive EV

click-chemistry labeling efficiency at the single-EV level. Unlike bulk fluorescence measurements, this approach allows the determination of click-chemistry labeling efficiency independently of fluctuations in total EV concentration by directly distinguishing Cy5-labeled from Cy5-unlabeled EV subpopulations at the single-particle level.

It should be noted that owing to the heterogeneity of CD63 expression levels among individual EVs, particles with surface markers below the system's limit of detection (LOD) remain uncounted. Nevertheless, for the EV subpopulation expressing CD63 above the LOD threshold, each vesicle is digitally registered as a single fluorescence event irrespective of its specific intensity, thereby ensuring reliable relative quantification of detectable CD63-positive EVs.

Effect of FBS concentration on EV yields and sample composition

Based on the dual-color detection profiles, we investigated the effect of fetal bovine serum (FBS) concentration in the culture medium during the final 24-h incubation. Tables 1 and 2 summarize the numbers of particles detected under 488-nm excitation only, 635-nm excitation only, and coincident dual excitation (488 and 635 nm) for HeLa and A549 cells, respectively. In this analysis, particles exhibiting either fluorescence under 488-nm excitation alone or under both 488- and 635-nm excitations were classified as CD63-positive EVs. Conversely, particles detected only under 635-nm excitation were classified as Cy5-labeled, CD63-negative particles, and these likely consisted either of cellular debris or non-EV membranous vesicles that retained the Cy5 label introduced by cell-surface click chemistry.

As shown in Tables 1 and 2, both cell lines produced the greatest number of EVs when cultured in medium supplemented with 10% FBS. In HeLa cells, the numbers of all particle populations varied with FBS concentration. Although the difference in the number of Cy5-labeled, CD63-negative particles between the 0 and 5% FBS conditions was not visually apparent, it was statistically significant ($p = 0.013$, Student's t-test). In a similar manner, A549 cells showed no significant differences in either the numbers of Cy5-labeled, CD63-positive EVs or Cy5-labeled, CD63-negative particles between the 0 and 5% FBS conditions, whereas significant differences were observed between the 5 and 10% FBS conditions and between the 10 and 15% FBS conditions.

These results suggest that the production of both CD63-positive EVs and Cy5-labeled, CD63-negative particles is influenced by the FBS concentration in the culture medium, which possibly reflects changes in the metabolic activity of the donor cells. Notably, the highest numbers of total EVs and click-chemistry-labeled EVs were obtained under the 10% FBS condition for both cell lines. These findings further suggest that sufficient EV production is important for recovering a detectable population of click-chemistry-labeled EVs under the present experimental conditions.

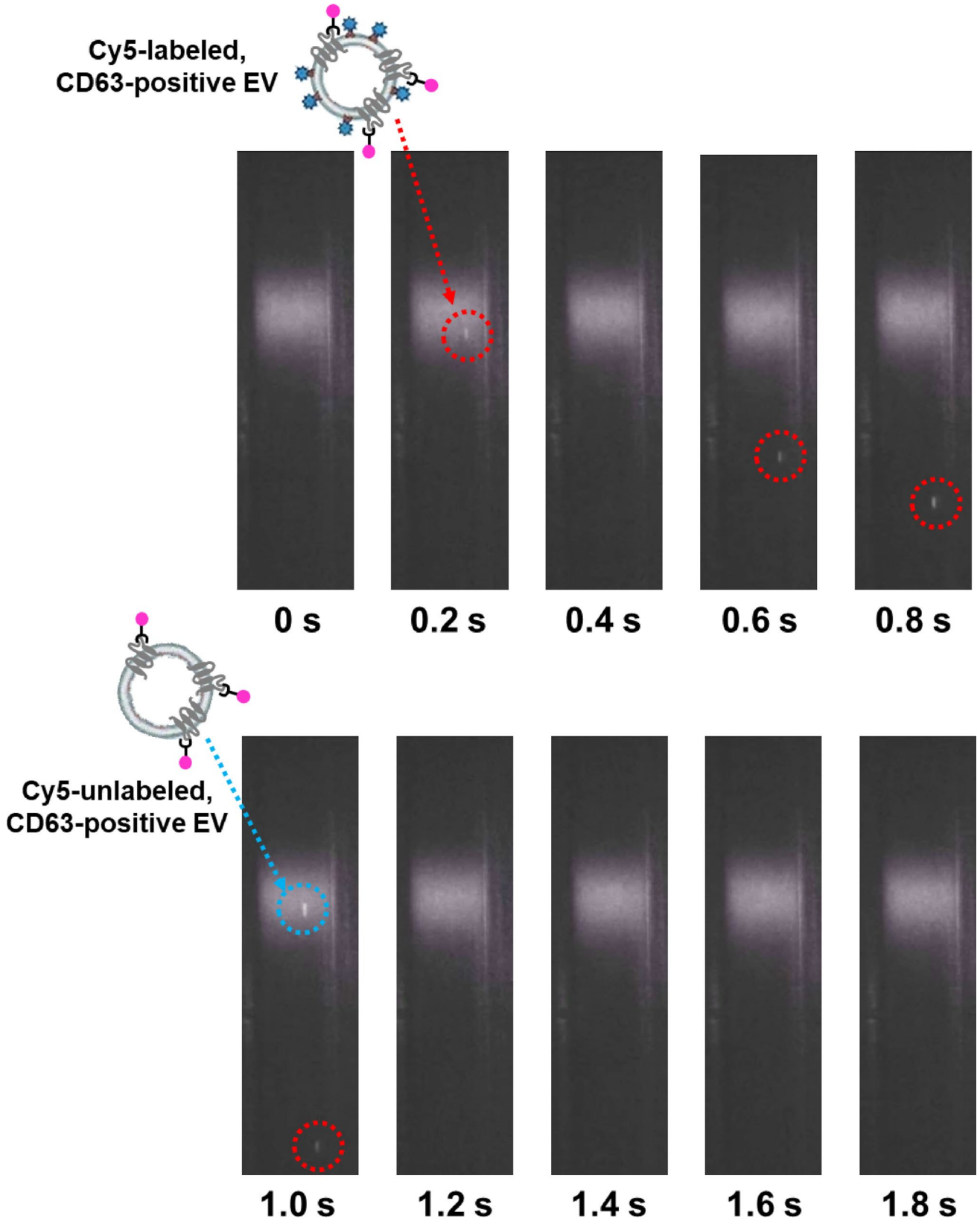


Fig. 4 Images of detecting Cy5-labeled, CD63-positive EV and Cy5-unlabeled, CD63-positive EV (labeled and unlabeled by bioorthogonal click chemistry)

Table 1 Average numbers of EVs released from HeLa cells cultured in media with different concentrations of fetal bovine serum

Volume fraction of fetal bovine serum/ %	Emissions only at 488-nm excitation (Cy5-unlabeled, CD63-positive EVs)	Emissions both at 488-nm and 635 nm excitation (Cy5-labeled, CD63-positive EVs)	Emissions only at 635 nm excitation (Cy5-labeled, CD63-negative particles)
0	451 ± 72 (98.0%)	7 ± 3 (2%)	2 ± 1 (0.4%)
5	451 ± 118 (89.0%)	51 ± 21 (10%)	5 ± 3 (1%)
10	674 ± 115 (78.5%)	163 ± 23 (19.0%)	22 ± 2 (2.5%)
15	268 ± 33 (93.4%)	16 ± 4 (5.6)	3 ± 3 (1%)

Measurement time, 10 min ($n = 5$). The values indicate the mean ± standard deviation. The values in parentheses are the percentages against the total number of the detected vesicles

Table 2 Average numbers of EVs released from A549 cells cultured in the media with different concentrations of fetal bovine serum

Volume fraction of fetal bovine serum/ %	Emissions only at 488-nm excitation (Cy5-unlabeled, CD63-positive EVs)	Emissions at 488-nm and 635 nm excitations (Cy5-labeled, CD63-positive EVs)	Emissions only at 635 nm excitation (Cy5-labeled, CD63-negative particles)
0	101 ± 28 (100%)	0 ± 0 (0%)	0 ± 0 (0%)
5	137 ± 26 (100%)	0 ± 0 (0%)	0 ± 0 (0%)
10	378 ± 93 (96.2%)	10 ± 3 (2.5%)	5 ± 3 (1%)
15	77 ± 31 (97%)	1 ± 1 (1%)	1 ± 1 (1%)

Measurement time: 10 min ($n = 5$). The values indicate the mean ± standard deviation. The values in parentheses are the percentages against the total number of detected vesicles

The proportion of Cy5-labeled EVs varied depending on the FBS concentration. Because metabolic labeling with the synthetic sugar precursor was completed prior to exposing cells to varying FBS conditions, this observation is unlikely due to direct modulation of initial precursor incorporation. Instead, it can be attributed to serum-dependent modulation of cellular metabolic activity, EV biogenesis pathways, and membrane trafficking during the EV secretion phase. Serum components supply nutrients and growth factors that stimulate cellular proliferation, endocytic/exocytic dynamics, and the turnover of cell-surface glycoproteins [21, 22]. Consequently, fluctuations in FBS concentration may alter the relative trafficking and sorting efficiency of pre-labeled membrane glycoproteins into secreted EVs compared to newly synthesized, unlabeled proteins, thereby potentially shifting the resultant proportion of Cy5-labeled EVs.

Evaluation of click-chemistry labeling efficiency and cell-line dependency

To quantitatively assess the performance of the metabolic modification, the labeling efficiency was defined as the ratio of Cy5-labeled, CD63-positive EVs to the total number of CD63-positive EVs. Under the optimal 10% FBS conditions, which provided the maximum EV yield, the labeling efficiency for HeLa cells was estimated to be 19.0%. Although ExoQuick-TC is a widely used commercial reagent that isolates EVs based on polymer-mediated precipitation, our dual-color platform revealed that the collected samples predominantly consisted of Cy5-unlabeled, CD63-positive EVs. This result implies that 19% of the total CD63-positive EVs recovered by ExoQuick-TC are successfully modified via this cell-surface click-chemistry approach.

It should be noted that the reported labeling percentage (19.0% in HeLa cells) represents the proportion of CD63-positive EVs with Cy5 fluorescence above the detection threshold, rather than the absolute chemical labeling efficiency of individual surface glycans. This value is influenced by the detection limit of the optics and the natural heterogeneity of glycan expression among CD63-positive EV subpopulations.

It is also important to note that the labeling efficiency of the click chemistry reaction on the cells themselves cannot be assumed to be 100%, which owes to variations in precursor conversion and to the reaction kinetics of cell membranes. Furthermore, the labeling percentages reported in this study are derived specifically from the CD63-positive EV population (vesicles with CD63 density above the detection limit) and do not account for either CD63-negative or CD63-low vesicles. Rather than serving as an absolute measure of total cell-surface reaction efficiency, our two-color analytical platform enables a quantitative comparison of metabolic precursor incorporation within specific, marker-defined EV subpopulations at the single-particle level.

When comparing the two cell lines under 10% FBS conditions, the total number of detected EVs for A549 cells (393) was drastically lower than that for HeLa cells (859). Furthermore, the labeling efficiency for A549 cells was only 2.5%, which is a sharp contrast to the 19.0% observed for HeLa cells. A Student's t-test based on five replicate

measurements confirmed that this discrepancy in labeling efficiency between HeLa and A549 cells was statistically highly significant ($p=0.0014$ at a 95% confidence level). These results suggest that click chemistry-based labeling efficiency is cell-line dependent [23]. The observed differences in both the number of detected EVs and labeling efficiency could reflect intrinsic biological differences between HeLa and A549 cells.

The observation that a major proportion of CD63-positive EVs remained Cy5-unlabeled (e.g., ~81% in HeLa cells and ~97.5% in A549 cells) highlights the inherent heterogeneity of metabolic labeling among vesicles. While direct measurement of precursor spatial uniformity on live cell membranes remains technically challenging, several factors likely account for these relatively low labeling proportions.

First, distinct EV biogenesis pathways—such as direct budding from the plasma membrane versus endosomal sorting via multivesicular bodies—yield vesicles with inherently different membrane compositions. Second, non-uniform distribution of target glycans within cell membrane microdomains could cause unequal precursor packaging during vesicle formation. Finally, vesicles with precursor incorporation levels below the optical detection threshold are classified as Cy5-negative. These findings emphasize the utility of single-vesicle analysis in uncovering population-level labeling dynamics that remain hidden in bulk measurements.

One possible explanation for the observed differences in both the number of detected EVs and labeling efficiency is the intrinsic biological characteristics of the two cell lines. HeLa cells are characterized by rapid proliferation and high levels of metabolic activity, which previous studies have associated with enhanced membrane trafficking and EV biogenesis [24–26]. Consequently, under identical culture conditions, HeLa cells could produce a greater number of CD63-positive EVs compared with that produced by A549 cells. In addition, cell-line-specific differences in the expression of key regulators of EV biogenesis and secretion, including endosomal sorting complex required for transport (ESCRT) components and Rab GTPases (e.g., Rab27a and Rab27b), could also contribute to the observed differences in EV production [27]. Furthermore, because click chemistry-based labeling relies on the metabolic incorporation of azide-containing glycoconjugates into newly synthesized membrane components, differences in cellular metabolic activity and membrane turnover could also influence labeling efficiency. Together, these factors support the higher EV yield and labeling efficiency observed in HeLa cells compared with that in A549 cells.

Conclusions

In this study, we developed a quantitative platform for evaluating the efficiency of click chemistry-based EV labeling using a two-color laser-induced fluorometry (LIF) system. Although previous studies employed serum-free culture conditions, our results demonstrated that supplementation of the culture medium with 10% fetal bovine serum (FBS) provided the highest yield of detectable EVs under the present experimental conditions. By combining dual-laser fluorescence detection with PE-anti-CD63 staining, the proposed system successfully distinguished Cy5-labeled, CD63-positive EVs from Cy5-unlabeled, CD63-positive EVs.

Quantitative analysis showed that 19.0% of CD63-positive EVs released from HeLa cells were successfully labeled with Cy5, whereas the corresponding labeling efficiency for A549 cells was only 2.5%, which demonstrates a marked degree of cell-line dependence. This difference is likely attributable to intrinsic biological differences between the two cell lines that influence EV production and labeling efficiency.

Compared with conventional single-EV platforms, the present method offers distinct technical and practical advantages. High-sensitivity flow cytometry, while capable of single-particle analysis, requires specialized and costly instrumentation. Our strategy circumvents this limitation by enabling direct, cost-effective measurement of culture media.

Furthermore, while antibody-functionalized array devices capture EVs via surface markers, detection that relies solely on target-derived fluorescence (e.g., Cy5) fails to visualize unlabeled vesicles. Consequently, such array approaches can be used neither to evaluate a non-labeled subpopulation nor to quantify the absolute labeling proportion. By simultaneously detecting both CD63 expression and Cy5 labeling at the single-vesicle level, our platform overcomes this blind spot and provides an accurate, quantitative assessment of the proportion of labeled EVs within a specific EV population.

The proposed two-color LIF platform enables quantitative, single-particle evaluation of click chemistry-based EV labeling efficiency. This approach should be useful for optimizing EV functionalization strategies and could be used to facilitate the future development of EV-based drug delivery systems and diagnostic technologies.

Acknowledgements This work was supported by Japan Society for Promotion of Science (JSPS) KAKENHI Grant Number JP25K01800.

Author contributions Arisa Takaya: Methodology, Validation, Formal analysis, Investigation, Data curation, Visualization. Takashi Kaneta: Conceptualization, Methodology, Formal analysis, Resources, Data curation, Writing—review & editing, Writing—original draft, Visualization, Supervision, Project administration. Funding acquisition.

Funding Open Access funding provided by Okayama University

Data availability Data will be made available upon request.

Declarations

Conflict of interest The authors declare that they have no known competing financial interests or personal relationships that could appear to influence the work reported in this paper.

Open Access This article is licensed under a Creative Commons Attribution 4.0 International License, which permits use, sharing, adaptation, distribution and reproduction in any medium or format, as long as you give appropriate credit to the original author(s) and the source, provide a link to the Creative Commons licence, and indicate if changes were made. The images or other third party material in this article are included in the article's Creative Commons licence, unless indicated otherwise in a credit line to the material. If material is not included in the article's Creative Commons licence and your intended use is not permitted by statutory regulation or exceeds the permitted use, you will need to obtain permission directly from the copyright holder. To view a copy of this licence, visit http://creativecommons.org/licenses/by/4.0/.

References

1. H. Valadi, K. Ekström, A. Bossios, M. Sjöstrand, J.J. Lee, J.O. Lötvall, Exosome-mediated transfer of mRNAs and microRNAs is a novel mechanism of genetic exchange between cells. Nat. Cell. Biol. **9**, 654–659 (2007). https://doi.org/10.1038/ncb1596
2. C. Kahlert, S.A. Melo, A. Protopopov, J. Tang, S. Seth, M. Koch, J. Zhang, W. Weitz, L. Chin, A. Futreal, R. Kalluri, Identification of double-stranded genomic DNA spanning all chromosomes with mutated KRAS and p53 DNA in the serum exosomes of patients with pancreatic cancer. J. Biol. Chem. **289**, 3869–3875 (2014). https://doi.org/10.1074/jbc.C113.532267
3. B. Thakur, H. Zhang, A. Becker, I. Matei, Y. Huang, B. Costa-Silva, H. Peinado, H. Shih, D. Lyden, Double-stranded DNA in exosomes: a novel biomarker in cancer detection. Cell. Res. **24**, 766–769 (2014). https://doi.org/10.1038/cr.2014.44
4. S.A. Melo, L.B. Luecke, C. Kahlert, A.F. Fernandez, S.T. Gammon, J. Kaye, V.S. LeBleu, E.A. Mittendorf, J. Weitz, N. Rahbari, C. Reissfelder, C. Pilarsky, M.F. Fraga, D. Piwnica-Worms, R. Kalluri, Glypican-1 identifies cancer exosomes and detects early pancreatic cancer. Nature. **523**, 177–182 (2015). https://doi.org/10.1038/nature14581
5. A. Hoshino, B. Costa-Silva, T.L. Shen, G. Rodrigues, A. Hashimoto, M. Tesic Mark, H. Molina, S. Kohsaka, Di A. Giannatale, S. Ceder, S. Singh, C. Williams, N. Soplop, K. Uryu, L. Pharmer, T. King, L. Bojmar, A.E. Davies, Y. Ararso, T. Zhang, H. Zhang, J. Hernandez, J.M. Weiss, V.D. Dumont-Cole, K. Kramer, L.H. Wexler, A. Narendran, G.K. Schwartz, J.H. Healey, P. Sandstrom, K.J. Labori, E.H. Kure, P.M. Grandgenett, M.A. Hollingsworth, de M. Sousa, S. Kaur, M. Jain, K. Mallya, S.K. Batra, W.R. Jarnagin, M.S. Brady, O. Fodstad, V. Müller, K. Pantel, A.J. Minn, M.J. Bissell, B.A. Garcia, Y. Kang, V.K. Rajasekhar, C.M. Ghajar, I. Matei, H. Peinado, J. Bromberg, D. Lyden, Tumour exosome integrins determine organotropic metastasis. Nature. **527**, 329–335 (2015). https://doi.org/10.1038/nature15756
6. R. Kalluri, V.S. LeBleu, The biology, function, and biomedical applications of exosomes. Science. **367**, eaau6977 (2020). https://doi.org/10.1126/science.eaau6977
7. C. Théry, S. Amigorena, G. Raposo, A. Clayton, Isolation and characterization of exosomes from cell culture supernatants and biological fluids. Curr. Protoc. Cell. Biol. Chapter 3, Unit 3.22 (2006). https://doi.org/10.1002/0471143030.cb0322s30
8. R.A. Dragovic, C. Gardiner, A.S. Brooks, D.S. Tannetta, D.J. Ferguson, P. Hole, B. Carr, C.W. Redman, A.L. Harris, P.J. Dobson, P. Harrison, I.L. Sargent, Sizing and phenotyping of cellular vesicles using nanoparticle tracking analysis. Nanomedicine. **7**, 780–788 (2011). https://doi.org/10.1016/j.nano.2011.04.003
9. Y. Sato, K. Kuwahara, K. Mogami, K. Takahashi, S. Nishizawa, Amphipathic helical peptide-based fluorogenic probes for a marker-free analysis of exosomes based on membrane-curvature sensing. RSC Adv. **10**, 38323–38327 (2020). https://doi.org/10.1039/d0ra07763a
10. M. Dehghani, S.M. Gulvin, J. Flax, T.R. Gaborski, Systematic evaluation of PKH labelling on extracellular vesicle size by Nanoparticle Tracking Analysis. Sci. Rep. **10**, 9533 (2020). https://doi.org/10.1038/s41598-020-66434-7
11. T. Tian, Y. Wang, H. Wang, Z. Zhu, Z. Xiao, Visualizing of the cellular uptake and intracellular trafficking of exosomes by live-cell microscopy. J. Cell. Biochem. **111**, 488–496 (2010). https://doi.org/10.1002/jcb.22733
12. T. Smyth, K. Petrova, N.M. Payton, I. Persaud, J.S. Redzic, M.W. Graner, P. Smith-Jones, T.J. Anchordoquy, Surface functionalization of exosomes using click chemistry. Bioconjug. Chem. **25**, 1777–1784 (2014). https://doi.org/10.1021/bc500291r
13. S. Song, M.K. Shim, S. Lim, Y. Moon, S. Yang, J. Kim, Y. Hong, H.Y. Yoon, I.S. Kim, K.Y. Hwang, K. Kim, In situ one-step fluorescence labeling strategy of exosomes via bioorthogonal click chemistry for real-time exosome tracking in vitro and in vivo. Bioconjug. Chem. **31**, 1562–1574 (2020). https://doi.org/10.1021/acs.bioconjchem.0c00216
14. Z. Li, Y. Liu, F. Liu, G. Sun, X. Zhang, J. Jing, Bioorthogonal click chemistry and aptamer-targeting enables highly selective fluorescence labeling of exosomal glycosylated EpCAM for super resolved imaging. Anal. Chim. Acta. **1339**, 343623 (2025). https://doi.org/10.1016/j.aca.2025.343623
15. N. Mukerjee, S. Maitra, M. Kaur, M.M. Rekha, P. Soothwal, I. Arora, N.D. Thorat, P.K. Sharma, A. Kaushik, Click chemistry-based modified exosomes: towards enhancing precision in cancer theranostics. Chem. Eng. J. **512**, 160915 (2025). https://doi.org/10.1016/j.cej.2025.160915
16. S. Asahi, T. Kaneta, Discrimination of nanovesicles using two-color laser-induced fluorescence detection. Spectrochim Acta Mol. Biomol. Spectrosc. **359**, 127928 (2026). https://doi.org/10.1016/j.saa.2026.127928
17. K.M. Danielson, J. Estanislau, J. Tigges, V. Toxavidis, V. Camacho, E.J. Felton, J. Khoory, S. Kreimer, A.R. Ivanov, P.Y. Mantel, J. Jones, P. Akuthota, S. Das, I. Ghiran, diurnal variations of circulating extracellular vesicles measured by nano flow cytometry. PLoS One. **11**, e0144678 (2016). https://doi.org/10.1371/journal.pone.0144678
18. Z.Y. Dong, H.C. Chen, X.Y. Qin, H.Q. Zheng, J. Gong, J. Chen, J.B. Zhang, W.J. Duan, Primer exchange reaction-based dual-signal amplified nano-flow cytometry and fluorescence analysis of MUC1-positive exosomes. Talanta. **311**, 130266 (2027). https://doi.org/10.1016/j.talanta.2026.130266
19. T. Fujii, T. Kaneta, Direct counting of exosomes in a cell culture medium using neither isolation nor preconcentration. Anal. Chim. Acta. **1119**, 35–40 (2020). https://doi.org/10.1016/j.aca.2020.04.052
20. J. Lötvall, A.F. Hill, F. Hochberg, E.I. Buzás, Di D. Vizio, C. Gardiner, Y.S. Gho, I.V. Kurochkin, S. Mathivanan, P. Quesenberry, S. Sahoo, H. Tahara, M.H. Wauben, K.W. Witwer, C. Théry, Minimal experimental requirements for definition of extracellular vesicles and their functions: a position statement from the

International Society for Extracellular Vesicles. J. Extracell. Vesicles. **3**, 26913 (2014). https://doi.org/10.3402/jev.v3.26913
21. J. Du, M.A. Meledeo, Z. Wang, H.S. Khanna, K.J. Paruchuri, Yarema, Metabolic glycoengineering: sialic acid and beyond. Glycobiology. **19**, 1382–1401 (2009). https://doi.org/10.1093/glycob/cwp115
22. K. Dammen-Brower, E. Tan, R.T. Almaraz, J. Du, K.J. Yarema, Protocol considerations for in vitro metabolic glycoengineering of non-natural glycans. Curr. Protoc. **3**, e822 (2023). https://doi.org/10.1002/cpz1.822
23. Y. Yoshioka, Y. Konishi, N. Kosaka, T. Katsuda, T. Kato, T. Ochiya, Comparative marker analysis of extracellular vesicles in different human cancer types. J. Extracell. Vesicles. **2**, 20424 (2013). https://doi.org/10.3402/jev.v2i0.20424
24. H.W. King, M.Z. Michael, J.M. Gleadle, Hypoxic enhancement of exosome release by breast cancer cells. BMC Cancer. **12**, 421 (2012). https://doi.org/10.1186/1471-2407-12-421
25. S.V. Chitti, P. Fonseka, S. Mathivanan, Emerging role of extracellular vesicles in mediating cancer cachexia. Biochem. Soc. Trans. **46**, 1129–1136 (2018). https://doi.org/10.1042/BST20180213
26. M. Colombo, C. Moita, van G. Niel, J. Kowal, J. Vigneron, P. Benaroch, N. Manel, L.F. Moita, C. Théry, G. Raposo, Analysis of ESCRT functions in exosome biogenesis, composition and secretion highlights the heterogeneity of extracellular vesicles. J. Cell. Sci. **126**, 5553–5565 (2013). https://doi.org/10.1242/jcs.128868
27. S. Nambara, T. Masuda, K. Hirose, Q. Hu, T. Tobo, Y. Ozato, J. Kurashige, Y. Hiraki, Y. Hisamatsu, T. Iguchi, K. Sugimachi, E. Oki, T. Yoshizumi, K. Mimori, Rab27b, a regulator of exosome secretion, is associated with peritoneal metastases in gastric cancer. Cancer Genomics Proteom. **20**, 30–39 (2023). https://doi.org/10.21873/cgp.20362

Publisher's note Springer Nature remains neutral with regard to jurisdictional claims in published maps and institutional affiliations.